Brain, Behavior, & Immunity - Health 7 (2020) 100116

Contents lists available at ScienceDirect

Brain, Behavior, & Immunity - Health

journal homepage: www.editorialmanager.com/bbih/default.aspx

Full Length Article

Deletion of indoleamine 2,3 dioxygenase (Ido)1 but not Ido2 exacerbates disease symptoms of MOG_{35-55}-induced experimental autoimmune encephalomyelitis

Lisa A. Wetzel [a], Myrna Hurtado [a,c], Zoe A. MacDowell Kaswan [b,c], Robert H. McCusker [a,b,c,d], Andrew J. Steelman [a,b,c,e,f,*]

[a] Department of Animal Sciences, University of Illinois at Urbana-Champaign, Urbana, IL, 61801, USA
[b] Neuroscience Program, University of Illinois at Urbana-Champaign, Urbana, IL, 61801, USA
[c] Integrative Immunology and Behavior Program, University of Illinois at Urbana-Champaign, Urbana, IL, 61801, USA
[d] Department of Pathology, University of Illinois at Urbana-Champaign, Urbana, IL, 61801, USA
[e] Division of Nutritional Sciences, Urbana-Champaign, Urbana, IL, 61801, USA
[f] Carl R. Woese Institute for Genomic Biology at Urbana-Champaign, Urbana, IL, 61801, USA

ARTICLE INFO

Keywords:
Indoleamine 2,3 dioxygenase
Experimental autoimmune encephalomyetlitis
Multiple sclerosis
Neuroinflammation

ABSTRACT

Multiple sclerosis (MS) is an autoimmune disease of the central nervous system (CNS) with pathological features of inflammation, demyelination, and neurodegeneration. Several lines of evidence suggest that the enzymes indoleamine 2,3-dioxygenase (Ido)1 and/or Ido2 influences susceptibility to autoimmune diseases. Deletion of *Ido1* exacerbates experimental autoimmune encephalomyelitis (EAE) an animal model of MS. However, no data exist on the role of *Ido2* in the pathogenesis of EAE. We investigated whether deletion of *Ido2* affected the pathogenesis of EAE. Temporal expression of interferon gamma (*Ifng*), *Ido1* variants, *Ido2* variants, as well as genes encoding enzymes of the kynurenine pathway in the spleen and spinal cord of C57BL/6 mice with or without EAE were determined by RT-qPCR. Moreover, EAE was induced in C57BL/6, two *Ido1* knockout strains ($Ido1^{KO}$ and $Ido1^{TK}$) and one Ido2 knockout mouse strain ($Ido2^{-/-}$) and disease monitored by clinical scores and weight change. Performance on the rotarod was performed on days 0, 5, 10 and 15 post induction. The extent of demyelination in the spinal cord was determined after staining with Oil red O. The development of EAE altered gene expression in both the spleen and spinal cord. Deletion of *Ido1* exacerbated the clinical symptoms of EAE. In stark contrast, EAE in $Ido2^{-/-}$ mice did not differ clinically or histologically from control mice. These results confirm a protective role for *Ido1*, on the pathogenesis of MOG_{35-55}-induced EAE in C57BL/6J mice.

1. Introduction

Multiple sclerosis (MS) is a CNS-restricted disease with pathological features of inflammation, demyelination, and neurodegeneration. Disease onset usually occurs in the second or third decade of life. In most cases, the natural history of MS is characterized by two phases: a relapsing-remitting phase during which the patient experiences periods of transient neurological dysfunction followed by periods of reprieve; and a secondary progressive phase characterized by prominent neurodegeneration and continual loss of function without remission. The etiology of MS is suspected to be multifactorial, with both genetic predisposition and environment contributing to disease onset (Compston and Coles, 2008).

Regardless of etiology, MS is considered an autoimmune disease. Indeed, the role of T and B cells in the pathogenesis and progression of MS is exemplified by the success of disease modifying agents that either deplete these cell types or inhibit their trafficking to the CNS (Miller et al., 2003; Hauser et al., 2008). Since the cause of MS remains elusive, no single animal model completely mimics the pathogenesis or natural history of the human disease. However, several clinical and pathological features of MS are recapitulated in the EAE model, whereby immunization of animals with myelin-specific antigens emulsified in Freund's adjuvant exhibit progressive neurological disease that is driven by autoreactive T and B cell responses. For these reasons, EAE is the most commonly used model with which to study autoimmune-mediated inflammatory demyelination.

* Corresponding author. Department of Animal Sciences, University of Illinois at Urbana-Champaign, Urbana, IL, 61801, USA.
E-mail address: asteelma@illinois.edu (A.J. Steelman).

https://doi.org/10.1016/j.bbih.2020.100116
Received 21 July 2020; Accepted 23 July 2020
Available online 25 July 2020

The enzymes indoleamine 2,3 dioxygenases (IDO1 and IDO2) and tryptophan 2,3 dioxygenase (TDO2) catalyze the metabolism of L-tryptophan (Trp) to N-formyl-kynurenine then kynurenine (KYN), thereby initiating the kynurenine pathway. Activation of this enzymatic cascade generates metabolites which serve either neuroprotective (kynurenic acid) or neurotoxic (quinolinic acid) roles, but also act to regulate immune responses (Lovelace et al., 2016). Expression of IDOs is highly induced by type I (IFN-α, IFN-β) and type II (IFN-γ) interferons, both of which suppress disease activity in EAE (Willenborg et al., 1999; Inoue et al., 2012). Upregulation of IDO1, specifically is associated with a reduction in intracellular Trp (Yeung et al., 2012; Ganesan and Roy, 2019) and Trp depletion negatively impacts mTOR signaling (Munn and Mellor, 2013). Suppression of mTOR signaling by genetic or pharmacological manipulation inhibits the polarization and activation of encephalitogenic Th17 responses and ameliorates EAE (Donia et al., 2009; Esposito et al., 2010; Delgoffe et al., 2011; Koga et al., 2014; Hou et al., 2017). In addition to suppressing mTOR activity, intracellular Trp depletion activates the serine/threonine protein kinase general control non-derepressible 2 (GCN2) which in turn phosphorylates and inactivates eIF2α. Notably, GCN2 deficient mice also display exacerbated EAE (Orsini et al., 2014). Moreover, release of Kyn by antigen presenting cells suppresses effector immune responses and promotes Treg cell polarization by acting on the T cell aryl hydrocarbon receptor (AhR), thereby inhibiting autoimmune responses and resolving inflammation (Lippens et al., 2016). Indeed, mimicking the effect of Kyn by activation of the AhR with a novel agonist, gallic acid, ameliorates EAE (Abdullah et al., 2019). Transplantation of mesenchymal stem cells expressing *Ido1* alleviates body weight loss and clinical symptoms of MOG_{35-55}-induced EAE (Zhou et al., 2020). Finally, the relevance of Trp catabolism and kynurenine pathway activation by dioxygenases to the pathogenesis of human MS is illustrated by the findings that expression of IDO1 appears to correlate with disease activity (Mancuso et al., 2015) and that levels in peripheral blood mononuclear cells (PBMCs) from MS patients may be dysregulated (Negrotto and Correale, 2017). These data collectively suggest that perturbations in the kynurenine pathway may affect the pathogenesis of MS and that manipulation of this pathway may prove to be therapeutically efficacious in the treatment of MS or autoimmune diseases in general.

To date several studies demonstrate that *Ido1* and *Ido2* influence susceptibility to autoimmune diseases. For instance, pharmacological inhibition of IDO1 activity during EAE using 1-methyl-DL-tryptophan (1-MT) increased severity and histopathological scores of disease (Sakurai et al., 2002). Recent work by Lippens et al. demonstrated that of *Ido1* expression in plasmacytoid dendritic cells (pDC) was required to promote Treg cell expansion during the EAE priming phase and that deletion of *Ido1* in pDCs exacerbated EAE (Lippens et al., 2016). Interestingly, IDO2 has also been reported to affect immune responses in both IDO1 dependent and independent processes (Metz et al., 2019). Furthermore, IDO2 was shown to be a driver of autoreactive antibody generation and disease progression in a mouse model of rheumatoid arthritis (Merlo et al., 2014). Similarly, IDO2 was shown to exacerbate disease in an animal model of lupus (Merlo et al., 2016). As far as we are aware, no data exist on the role of IDO2 in the pathogenesis of EAE. Since B cells are critically involved in the pathogenesis of both MS (Hauser et al., 2008) and EAE (Parker Harp et al., 2015) we questioned whether global deletion of *Ido2* affected the clinical outcome of myelin associated glycoprotein (MOG_{35-55}) EAE in C57BL/6J mice. Herein we show that *Ido1*$^{-/-}$ mice exhibit exacerbated EAE, as previously reported by others. In stark contrast, EAE in *Ido2*$^{-/-}$ mice did not differ clinically or histologically from control mice indicating that *Ido2* has minimal, if any, effect on the pathogenesis of MOG_{35-55} induced EAE in C57BL/6J mice.

2. Methods and materials

2.1. Mice

Male mice aged 8–12 weeks were used for all experiments. C57BL/6J (Jackson Laboratories No. 000664), *Ido1* knockout (Ido1^{KO}; Jackson Laboratories No. 005867), in house Ido1 deficient Ido1^{TK} mice and *Ido2* deficient Ido2$^{-/-}$ mice are all on a C57BL/6J background.

Ido1 floxed (Ido1^{fl}) mice were generated by Drs. Keith W. Kelley and Robert Dantzer. A 75bp loxP cassette was inserted 5′ of the second exon of the reference gene NM_008324.2 (exon 3 in Suppl. Figure 1), by *ingenious targeting laboratory* (Ronkonkuma, NY). A second loxP site was inserted 3' of the fourth exon of NM_008324.2 (exon 5; Suppl. Fig. 1, *top*). Targeting was performed with C57BL/6 embryonic stem cells that were microinjected into Balb/c blastocysts. Chimeras with a black coat color were mated to C57BL/6 FLP mice to remove the Neo cassette. Cre recombinase excises a 2.37 kb region of the Ido1 gene. Knockout mice were generated by Dr. M^{c}Cusker by cross-breeding Ido1^{fl} mice to Cre^{+} mice to target *Ido1* inactivation in all cells, i.e. Total Knockout (Ido1^{TK}) mice. Ido1^{TK} mice were bred to C57BL/6 mice to remove the Cre gene and then the knockout allele was bred to homozygosity. The regions of the genome targeted for excision by Cre recombinase compared to the region deleted in Ido1 knockout (Ido1^{KO}) mice deposited for distribution by Andrew Mellor (Baban et al., 2004) available from JAX, 005867 is shown (Suppl. Fig. 1, *top*). Also shown is the relative position of the Ido2 gene, which is the next gene on chromosome 8 downstream of Ido1. Ido2$^{-/-}$ mice were a generous gift from Drs. Metz and Prendergast (Metz et al., 2019). Ido2$^{-/-}$ mice lack exon 9 and part of exon 10 of the reference gene NM_145949.2 (exons 10 and 11 in Suppl. Fig 1, *bottom*). Ido2$^{-/-}$ mice were supplied to Dr. McCusker with a Cre gene that was removed by breeding to C57BL/6 mice. The Ido2 knockout allele was then bred again to homozygosity.

All mice were group-housed in temperature- and humidity-controlled conditions and kept on a 12-h reversed light/dark cycle. Rodent diet (Teklad No. 8640) and water were provided *ad libitum*. At the end of each experiment, mice were anesthetized via intraperitoneal injection of ketamine (100 mg/kg) and xylazine (10 mg/kg). After reaching a surgical plane of anesthesia they were perfused through the heart with sterile phosphate buffer saline (PBS, pH 7.4) and their spinal cords and brains were extracted.

The experimental procedures described herein were approved by the Institutional Animal Care and Use Committee and were performed in accordance with guidelines of the National Institutes of Health.

2.2. Experimental autoimmune encephalomyelitis

Experimental autoimmune encephalomyelitis was induced using methods described previously (Lu et al., 2020). Specifically, complete Freund's Adjuvant (CFA) was generated by adding heat killed *Mycobacterium tuberculosis* H37 RA (MT; Difco, No. 231141) with incomplete Freund's adjuvant (Difco, No. 263910) to achieve a final concentration of 5 mg/ml. Equal volumes of MOG_{35-55} (Anaspec Inc.; 4 mg/ml) and the adjuvant mix were vortexed for 45 min. Mice were given four subcutaneous injections of MOG_{35-55}/adjuvant emulsion into the hind flanks. Finally, mice received an i.p. injection of sterile PBS containing 400 ng of pertussis toxin (List Biological Laboratories) on days 0 and again on day 2 post immunization. Disease was scored by raters blinded to genotype as described previously (Lu et al., 2020). Control (CFA) C57BL/6 mice were immunized with CFA in the absence of antigen.

2.3. Gene expression by real-time quantitative polymerase chain reaction (qPCR)

Control CFA mice (n = 5) were euthanized at day 15. EAE mice were euthanized at either the onset of disease (day 8; n = 5) or during peak disease (day 15; n = 5). Spinal cord and spleen were collected and either flash frozen in liquid nitrogen for qPCR or fixed in paraformaldehyde.

Frozen spinal cord and spleen were pulverized on dry ice using mortar and pestle. Samples (5–20 mg) were used for RNA isolation with E.Z.N.A. Total RNA Kit II (Omega Bio-tek, Norcross, GA) according to manufacturer's instructions; homogenization was achieved by sonication. RNA was quantified using the Nanodrop ND-1000 spectrophotometer

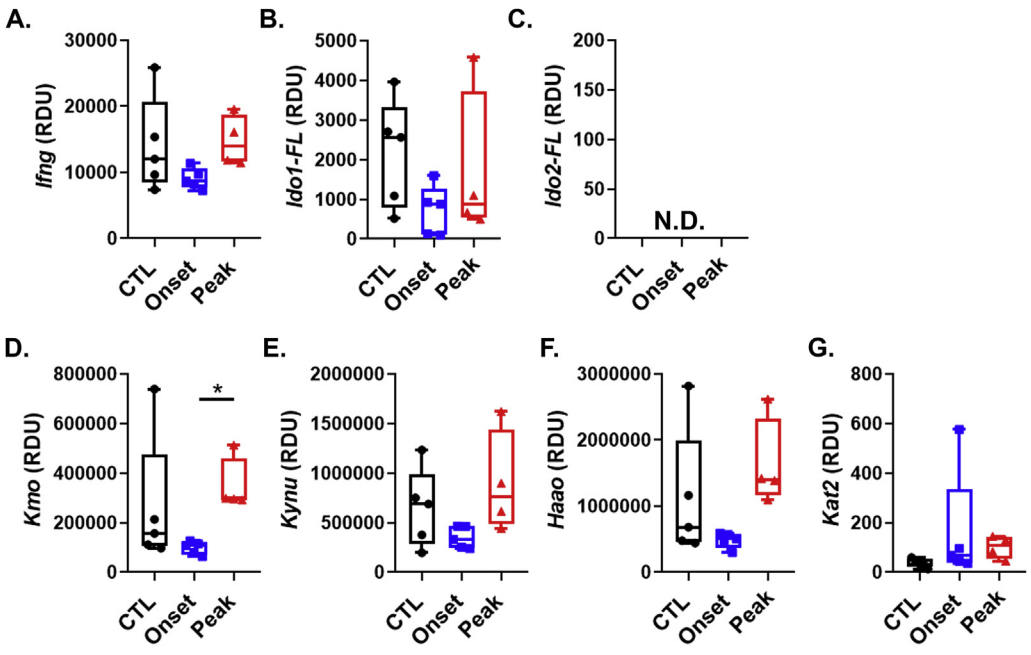

Fig. 1. Effect of EAE on the expression of *Ifng*, *Ido1*, *Ido2* and kynurenine pathway enzymes in the spleen. *A-G*, C57BL/6 mice were immunized with complete Freud's adjuvant (CFA) or MOG_{35-55} emulsified in CFA. Mice were euthanized at time points corresponding to disease onset (day 8) or during peak disease (day 15). Expression values for splenic *Ifng* **(A)**, *Ido1*-FL **(B)**, *Ido2*-FL **(C)**, *Kmo* **(D)**, *Kynu* **(E)**, *Haao* **(F)** and *Kat2* **(G)** were determined by real-time quantitative polymerase chain reaction. Results are expressed as box and whisker plots with individual data plotted for each mouse (n = 4–5 mice per group). $^*P < 0.05$.

(Thermo Scientific) and each sample was diluted to 50 ng/μl. Reverse transcription was performed using a High-Capacity cDNA Reverse Transcription Kit (Applied Biosystems) according to manufacturer instructions. The cDNA was diluted 10x in nuclease-free water for analysis. Each 10 μl qPCR reaction mixture contained 4.5 μl cDNA, 4.95 μl TaqMan master mix (PrimeTime Gene Expression Master Mix; IDT, Coralville, Iowa) and 0.55 μl probe-based assay. Real-time qPCR was performed in a QuantStudio 7 apparatus (Applied Biosystems). Data were normalized by the comparative threshold method ($\Delta C_t = C_t$ test transcript – C_t reference gene *Gapdh*). To calculate relative detection units (RDUs), ΔC_t values were normalized by setting the lowest detectable gene to 1.0 RDU. Thus, RDUs for every assay are relative to this 'reference' gene.' It is not proper to extrapolate RDU data as absolute differences in mRNA levels when comparing data across qPCR assays. However, presentation of the data in this manner permits visualization of the results for each mRNA species relative to all other isoforms or genes, providing an appreciation as to their relative abundance. These calculations were used to determine relative expression of *Ido1*, *Ido2,* their variants (Suppl. Fig. 1) as well as downstream Kyn pathway genes (*Kmo, Haao, Kynu, Kat2*) and *Ifng* using probe-based assays purchased from IDT (Coralville, Iowa) as described previously (Brooks et al., 2016a, 2016b, 2017; Dostal et al., 2017).

2.4. Rotarod analysis

Changes in balance and coordination were tested using a rotarod apparatus as this test is correlated with EAE disease progression (van den Berg et al., 2016). Mice were tested at days −3, 0, 5, 10 and 15 relative to immunization. Data were recorded on days 0, 5, 10 and 15. Because mice are nocturnal, each testing period occurred in the middle of their dark cycle. Each test day consisted of three trials for each mouse with each trial separated by a 15 min break. During the trial, mice were placed on the rotarod and duration of time on the rod was recorded. The apparatus increased speed at small increments, starting at 4 revolutions per minute (rpm) and reaching a maximum speed of 40 rpm. If a mouse fell from the apparatus, time was recorded and the mouse was placed back in its home cage. Mice that did not fall were allowed to run for a maximum of 300 s each trial. Notably, "flipping" (i.e. when a mouse hangs on to the rod while it is rotating) was not counted as falling, as it demonstrated grip strength and coordination. The average of all three trials were calculated per mouse at each time-point.

2.5. Histological evaluation of EAE pathology

Spinal cords were removed and fixed overnight at 4 °C with 4% paraformaldehyde (Acros Organics). The following day they were placed in a PBS solution containing 30% sucrose at 4 °C until they sank. Next, the spinal cords were cut into 6 sections, frozen in optimal cutting temperature solution (Tissue Tek, Torrence, CA) and sliced in transverse planes at a thickness of 18 μm using a cryostat (Leica CM1950). Visualization of myelin was achieved by staining for neutral lipids using Oil red O as described previously (Kim et al., 2012; Steelman et al., 2012). Unlike luxol fast blue, Oil red O is a lipophilic dye that stains lipid rather than lipoproteins present within myelin. Briefly, slides were rehydrated in phosphate buffered saline (pH 7.4) then incubated with propylene glycol for 2 min. The slides were placed in Oil red O solution for 24 h then washed with a solution of 80% propylene glycol/20% water. Slides were then scanned using a Nanozoomer (Hamamatsu) and scored by an experimenter blinded to genotype. The percentage of demyelination was quantified by tracing each lesion in the white matter of each section and dividing the total area of the lesions in that tissue by the total area of white matter for that tissue.

2.6. Statistical analysis

Statistical analyses were performed using GraphPad Prism version 7.0 or higher for Windows (GraphPad Software, La Jolla, CA). Normality was checked using the Shapiro–Wilk test. For parametric data, significant differences between groups were determined using one-way or two-way ANOVA followed by Bonferoni post hoc tests. For non-parametric data, significance was assessed by Kruskal-Wallis tests. Statistical significance was set at $p \leq 0.05$. Data are expressed as either whisker plots (interquartile ranges, upper/lower extremes plus medians) or means ± S.E.

3. Results

3.1. Ido1, but not Ido2, is upregulated in the spinal cord during EAE

Given that the expression of *Ido1* and *Ido2* have not been defined in models of EAE, we sought to quantify changes in their expression within the spleen and spinal cord tissues over the course of disease. Since IFN-γ is the strongest known inducer of *Ido1* expression and a prototypical marker of

EAE-induced neuroinflammation, we measured the expression of *Ifng* as well. Finally, expression levels of enzymes downstream of the Ido's involved in the Kyn pathway were determined. For these experiments, tissues were collected from C57BL/6 mice at the onset (days 8) and peak phases (day 15) of EAE. Tissues were also collected from control mice fifteen days after receiving CFA without antigen. The disease course for each group is shown in Suppl. Fig. 2A. Mice immunized with MOG_{35-55} emulsified in CFA displayed clinical signs of EAE. Disease onset was correlated with a marked increase in weight loss typical of EAE (Suppl. Fig. 2B).

Ifng was highly expressed in disease-free control (CTL) mouse spleens injected with Freund's adjuvant. However, its expression did not change as a result of EAE (Fig. 1A). We next quantified expression of the reference *Ido1* transcript. *Ido1-FL* was expressed in the spleen, but like *Ifng* did not change during the course of EAE (Fig. 1B). In contrast, the reference transcript for *Ido2*, *Ido2-FL,* was undetectable in CTL spleens and did not increase as a result of EAE (Fig. 1C). There are several alternate transcripts of murine *Ido1* and *Ido2*, their expression levels were also determined and shown (Suppl. Fig. 3). The Kyn pathway enzymes were highly expressed in the spleen. However, with the exception of *Kmo*, which was increased in the spleen during peak EAE compared to onset, there were no differences observed in the expression of the Kyn pathway *Kynu* and *Haao* (which act in tandem to generate quinolinic acid, QuinA, from Kyn, (Fig. 1D–F)). *Kat2*, which acts alone to generate kynurenic acid (KynA) from Kyn, was poorly expressed and non-inducible in the spleen (Fig. 2G). Given the high expression of *Kmo*, *Kynu* and *Haao* most of the Kyn generated may be shunted toward QuinA production, at least in the spleen.

In contrast to our observations in the spleen both *Ifng* and *Ido1-FL*, were poorly expressed in CTL spinal cords. However, their expression levels were strikingly elevated within the spinal cords of mice during peak EAE (Fig. 2A–B). The expression of *Ido2-FL* was undetectable and not altered in the spinal cord because of EAE (Fig. 2C). The effect of EAE on the spinal cord expression levels of alternative transcripts for *Ido1* and *Ido2* were also determined (Suppl. Fig. 4). Of the Kyn pathway genes assessed, levels of both *Kmo*, *Kynu* and *Haao* (Fig. 2D, E, F) were expressed at a considerably lower level when compared to spleen, whereas *Kat2* expression was higher (Fig. 2G). The peak phases of EAE was associated with and increased expression of *Kmo* and *Haao* in the spinal cord. These data indicate that *Ido1* is dramatically upregulated in the spinal cord during the peak phase of EAE and may affect lymphocyte effector function.

3.2. Deletion of Ido1 but not Ido2 affects the pathogenesis of EAE

Both IDO1 and IDO2 have been shown to be involved in the generation of autoimmune diseases. While full-length *Ido2* was not detectable at the transcriptional level in either the spleen or spinal cord during EAE we could not exclude its involvement in disease pathogensis. Therefore, we questioned if *Ido2* deletion influenced the pathogenesis of MOG_{35-55}-induced EAE. Since deletion of IDO1 is known to exacerbate EAE, conventional $Ido1^{KO}$ mice as well as a separate line generated in house ($Ido1^{TK}$) were used as positive controls. The incidence of EAE was 100% for both genotypes and disease progression was nearly identical in $Ido1^{KO}$ and $Ido1^{TK}$ mice (Suppl. Fig. 5). Therefore, mice from both of these groups were combined for all other analyses and are hence referred to simply as $Ido1^{-/-}$.

$Ido1^{-/-}$ mice exhibited exacerbated disease (Fig. 3A) and lost more weight (Fig. 3B) compared to either C57BL/6 or $Ido2^{-/-}$ mice. $Ido1^{-/-}$ mice achieved higher maximal EAE scores (Fig. 3C) and displayed an increased mortality rate (40%) compared to either WT (10%) or $Ido2^{-/-}$ (10%) mice (Fig. 3C; Score = 5). In stark contrast, the pathogenesis of EAE in *Ido2* knockout mice closely resembled that of C57BL/6 mice. Moreover, deletion of *Ido2* did not affect weight change or disease severity compared to C57BL/6 mice. There were no differences in time to disease onset across the mouse strains (Fig. 3D).

To further evaluate disease onset and severity, changes in overall motor skills (a sum of balance, coordination and strength) was assessed as rotarod performance at days 0, 5, 10 and 15 post immunization (p.i.). We found that all mice strains performed equally well at days 0 and 5 p.i. However, each strain exhibited a substantial decrease in performance at day 10 and 15 p.i. (Fig. 3E). The reduced performance at day 10 is intriguing since the majority of mice (37/42; 88%) did not exhibit clinical signs of EAE at this time-point. Nevertheless, we did not observe differences in motor skills attributable to genotype. These results indicate that rotarod performance is a sensitive objective measure for evaluating early subclinical symptoms of EAE.

3.3. Effect of Ido1 or Ido2 deletion on EAE-induced spinal cord demyelination

To determine if deletion of *Ido1* or *Ido2* affected the degree of spinal cord pathology, we assessed the percentage of demyelination in lumbar,

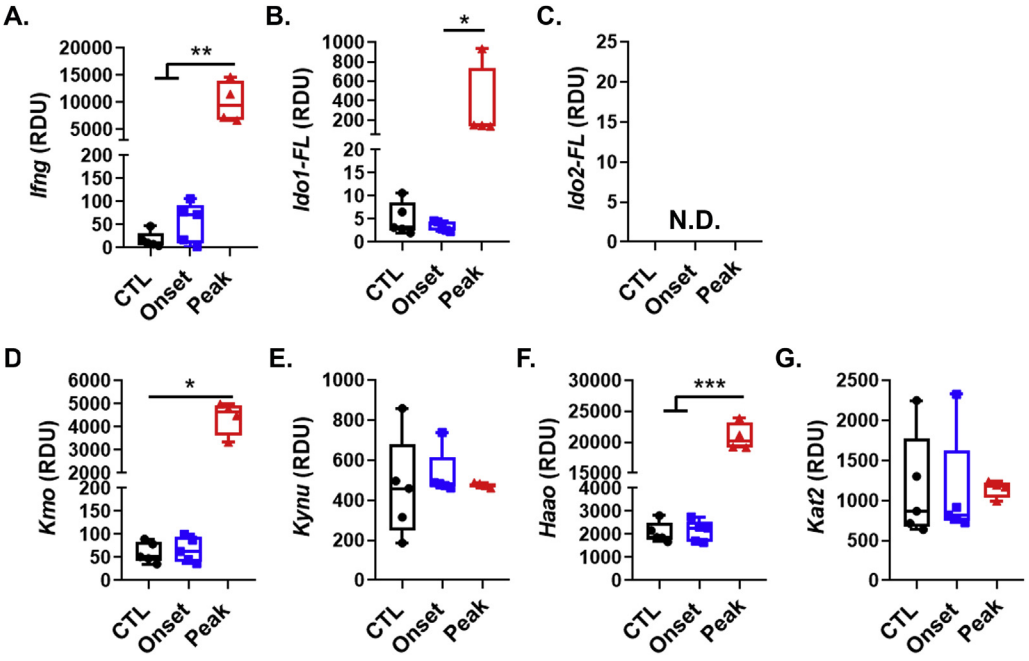

Fig. 2. Effect of EAE on the expression of *Ifng*, *Ido1*, *Ido2* and kynurenine pathway enzymes in the spinal cord. ***A-G,*** C57BL/6 mice were immunized with complete Freud's adjuvant (CFA) or MOG_{35-55} emulsified in CFA. Mice were euthanized at time points corresponding to disease onset (day 8) or during the peak disease (day 15). Expression values for splenic *Ifng* **(A)**, *Ido1*-FL **(B)**, *Ido2*-FL **(C)**, *Kmo* **(D)**, *Kynu* **(E)**, *Haao* **(F)** and *Kat2* **(G)** were determined by real-time quantitative polymerase chain reaction. Results are expressed as box and whisker plots with individual data plotted for each mouse (n = 4–5 mice per group). $^{*}P < 0.05$, $^{**}P < 0.001$, $^{***}P < 0.001$.

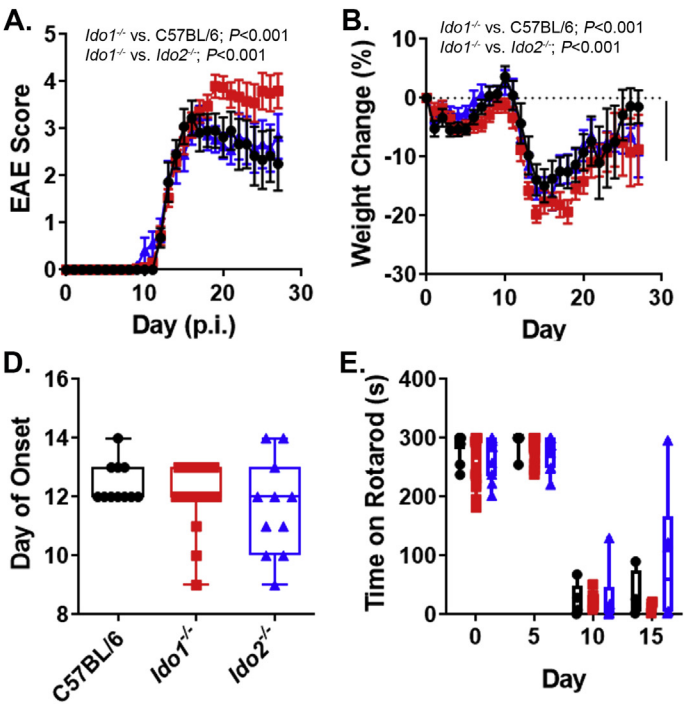

Fig. 3. EAE scores of *Ido1*$^{-/-}$ (Ido1^{KO} and Ido1^{TK} combined) but not *Ido2*$^{-/-}$ mice differ from control C57BL/6. ***A-D,*** Following induction of EAE, mice were weighed scored daily. The effect of mouse genotype on disease progression **(A),** weight change **(B)**, maximum score achieved **(C),** day of onset **(D)** and rotarod performance **(E)** are shown. Results are expressed as means ± S.E. or box and whisker plots with individual data plotted for each mouse. Numbers of mice per group are as follow: C57BL/6, n = 11; *Ido2*$^{-/-}$, n = 11 and *Ido1*$^{-/-}$, n = 20. Slope analysis was used to assess clinical scores. Differences in weights were assessed by ANOVA. Max score was analyzed using Kruskal-Wallis test. *$P < 0.05$.

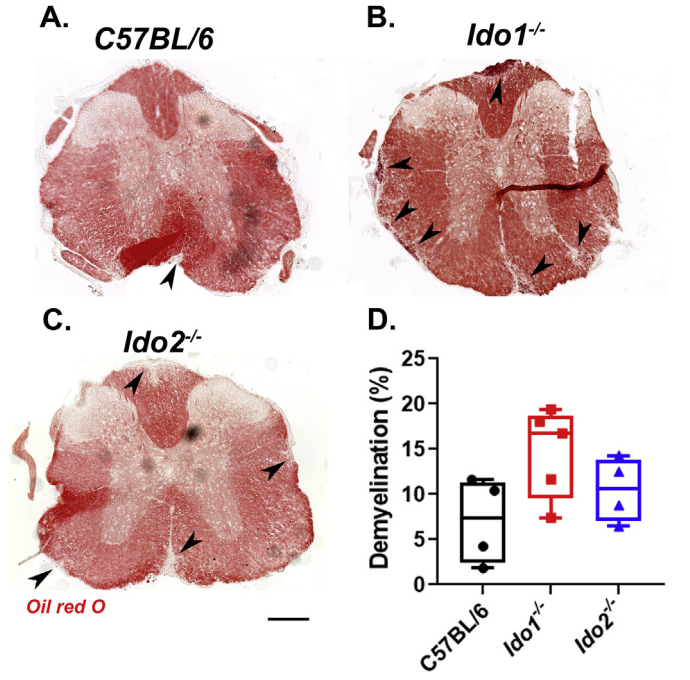

Fig. 4. The effect of genotype on spinal cord pathology following EAE induction. Spinal cord sections were stained with Oil Red O and demyelination percentage was quantified using ImageJ software. Representative thoracic sections of each genotype are shown. Average demyelination scores were taken from at least four mice per strain. The percentage of demyelination for each anatomical location was estimated by averaging results obtained from 3–5 sections per mouse. The values of all sections were averaged for each mouse. Therefore, each point represent the average lesion load expressed as the percentage of total white matter for individual mice. Scale bar = 200 μm. (For interpretation of the references to color in this figure legend, the reader is referred to the Web version of this article.)

thoracic and cervical sections after staining myelin with Oil red O. Consistent with our clinical observations, *Ido2* deletion had no effect on lesion size or percentage compared to C57BL/6 mice (Fig. 4). Induction of EAE in *Ido1* deficient mice appeared to exacerbate pathology compared to C57BL/6 mice, indicated by a slight increase in the percentage of spinal cord demyelination, but this effect did not reach statistical significance (Fig. 4D).

4. Discussion

The current experiments were designed to test the role of *Ido1* and *Ido2* during the pathogenesis of EAE. Our data show that *Ido1*$^{-/-}$ mice exhibit exacerbated clinical symptoms of EAE, characterized by greater weight loss during peak disease, an increase in maximal clinical score and a strong trend towards increased spinal cord pathology compared to C57BL/6 or *Ido2*$^{-/-}$ mice. In stark contrast, deletion of *Ido2* did not affect the clinical progression of EAE and spinal cord pathology did not differ between *Ido2*$^{-/-}$ mice and C57BL/6 mice. Rotarod performance decreased during EAE, an effect that preceded clinical symptoms, but did not differ across genotypes. Together, these data strongly indicate that *Ido2* deletion does not affect the onset or progression of MOG_{35-55}-dependent EAE, whereas *Ido1* has a protective role against disease progression.

In line with previous work (Sakurai et al., 2002; Kwidzinski et al., 2005; Matysiak et al., 2008; Mondanelli et al., 2020), data from the current study lend support for a protective role of *Ido1* by limiting autoimmune-mediated clinical severity in an animal model of MS. Specificity of the Ido1 response was illustrated by elevated expression of *Ido1-FL* in the spinal cord, but not the spleen. The qPCR assay assesses the steady-state level of exons (Compston and Coles, 2008; Miller et al., 2003; Hauser et al., 2008) that are necessary for expression the reference Ido1 transcript designated here as *Ido1-FL*. *Ido1-FL* encodes the enzymatically active IDO1 protein (IDO1-FL) and *Ido1-FL* expression is highly sensitive to IFN-γ signaling. Thus, *Ido1-FL* expression paralleled that of *Ifng*, which was also elevated in the spinal cord, but not the spleen. *Ido1-FL* expression likely results partially from IFN-γ-dependent induction within cells resident to the CNS such as microglia and astrocytes (Brooks et al., 2017; Dostal et al., 2018), but more importantly the

increase reflects neuroinflammation induced infiltration of immune cells. We have shown that murine PBMCs and T cells both respond to IFN-γ by increasing *Ido1-FL* expression (Brooks et al., 2017). The timing of *Ido1-FL* elevation in the current experiment corresponds to peak T cell infiltration (Lu et al., 2020). Independent of the cellular source, elevated *Ido1-FL* expression suggests enhanced Kyn production and thus AhR-mediated immunomodulation. In contrast to *Ido1-FL*, the major *Ido1* transcript in the mouse brain (*Ido1-v1*) (Brooks et al., 2016a; Dostal et al., 2017) encodes an enzymatically inactive IDO1 protein isoform (IDO1-v1(30). The Ido1-v1 RNA isoform was not induced in the spleen or spinal cord (Suppl. Figs. 3&4) by EAE. *Ido1-v2*, which also encodes the IDO1-v protein, however was induced in the spinal cord by EAE. Although, not enzymatically active, IDO1 protein have non-enzymatic immunosuppressive activity (Chen, 2011; Albini et al., 2017, 2018). A non-enzymatic role for the IDO1-v protein within the brain is currently under investigation. The greater expression of *Ido1-v1* relative to *Ido1-FL* (300:1) in the spinal cord, but similar ratio for *Ido1-FL*:*Ido1-v*1 expression within the spleen, suggests a unique function of IDO1-v1 in the nervous system.

In contrast to *Ido1*, *Ido2* expression, especially the transcript encoding the enzymatically active enzyme IDO2-FL, is very low in the spinal cord and spleen and not induced during EAE, at least at the time-points we measured. Thus, it was not necessarily surprising that *Ido2* deficiency did not alter EAE progression. *Ido2-FL* expression is absent in murine PBMCs and T cells (Brooks et al., 2017), thus its expression would not be expected to increase in parallel with immune cell infiltration into the spinal cord during EAE. Similar to *Ido1-FL* and *Ido1-v1* relative expression levels, expression of variant Ido2 transcripts is much higher in the spinal cord than is *Ido2-FL*. As for *Ido1-v1*, the role of these variant Ido2 transcripts and their encoded proteins within the CNS is unknown. However, all Ido2 transcripts are deficient in $Ido2^{KO}$ mice, suggesting that they are present but do not play a major role in MOG_{35-55}-induced EAE.

The importance of the immunoregulatory effects of IDO1, IDO2 and TDO2 in controlling PBMC responses in the context of MS were recently investigated by Negrotto and Correale (2017). Intriguingly, they found that IDO1 was downregulated in PBMCs obtained from MS patients compared to patients with other neurological diseases and healthy controls. Furthermore, myelin basic protein (MBP)-specific T cell lines from MS patients cultured in the presence of Trp and Arg were associated with decreased activation of GCN2, increased mTOR signaling and increased lymphocyte responsiveness to antigen stimulation. Conversely, the expression of *IDO2* and *TDO2* were not different between groups, indicating a potentially less important role for these enzymes in controlling immune responsiveness (Kim et al., 2012). Moreover, studies by Agliardi et al. failed to support an association between known functional SNPs (rs10109853 and rs4503083), which suppress *IDO2* expression and the onset or progression of MS (Agliardi et al., 2017). In contrast, Cha et al. found that both *IDO1* and *IDO2* expression was increased in acutely isolated and unstimulated PBMCs from MS patients compared to healthy controls or patients with clinically isolated syndrome (Cha et al., 2018). Together, these three studies demonstrate fluctuations in the transcription of enzymes involved in Trp metabolism that may be influenced by patient treatment status, genetic background or culture condition (Cha et al., 2018). Our work suggests that expression of *Ido1* rather than *Ido2* is needed to suppress symptoms of EAE following immunization with the MOG_{35-55} peptide. Since EAE is the prototypical antigen-specific autoimmune T cell-mediated disease, our data also suggest that *Ido2* does not play a non-redundant role in establishing T cell-mediated autoimmunity.

IDO2 is implicated as a driver of autoreactive antibody generation and disease progression in a mouse model of rheumatoid arthritis (Merlo et al., 2014). While our data clearly suggest that deletion of *Ido2* does not affect the pathogenesis of EAE, a potential caveat of our study was is that we did not specifically examine the effects of *Ido2* deletion on B cell effector functions, particularly with regards to antibody responses to MOG_{35-55}. The contribution of B cells to MS is clearly illustrated by the therapeutic efficacy of rituximab treatment, which depletes B cells and greatly suppresses relapses (Hauser et al., 2008). During MOG-induced EAE, B cells were shown to be required for sustained disease progression (Parker Harp et al., 2015; Barr et al., 2012). However, unlike animal models of rheumatoid arthritis, autoantibodies are not thought to contribute to EAE disease progression after immunization with myelin peptides such as MOG_{35-55} (Oliver et al., 2003). Instead, the contribution of B cells to the pathogenesis of EAE is likely attributable to their ability to present antigen to T cells (Parker Harp et al., 2015) or modulate immune function through the production of proinflammatory cytokines (Barr et al., 2012). Nevertheless, autoantibodies with specificity for neuroantigens are known to contribute to other neuroinflammatory, demyelinating diseases including neuromyelitis optica (NMO) and perhaps anti-MOG associated encephalomyelitis. Regarding NMO, injection of NMO patient-derived antibodies and human complement into the brains of healthy mice was has been found to be sufficient to cause demyelination (Saadoun et al., 2010). Given the role of Ido2 in autoantibody generation, it may be prudent for future investigations to query the association of this gene in either NMO or anti-MOG_{1-125} associated encephalomyelitis.

In conclusion, we have investigated the effects of *Ido1* and *Ido2* deletion on the pathogenesis of EAE, a widely used animal model of MS. Our data suggest that deletion of *Ido1* is associated with exacerbated disease. In contrast, deletion of Ido2 did not affect disease onset, symptomology or pathology. These data indicate *Ido2* does not have a major role in the pathogenesis of MOG_{35-55}-dependent EAE.

Declaration of competing interest

None.

Acknowledgement

The authors are grateful for funding provided to conduct the studies herein. This research was funded in part by the USDA National Institute of Food and Agriculture, HATCH Project ILLU-538-932 (A.J.S.), University of Illinois start-up funds (A.J.S), the National Multiple Sclerosis Society RG 1807-32053 (A.J.S.) and the National Institutes of Health 9R01NS106688-04 (R.H.M).

Appendix A. Supplementary data

Supplementary data to this article can be found online at https://doi.org/10.1016/j.bbih.2020.100116.

References

Abdullah, A., Maged, M., Hairul-Islam, M.I., Osama, I.A., Maha, H., Manal, A., Hamza, H., 2019. Activation of aryl hydrocarbon receptor signaling by a novel agonist ameliorates autoimmune encephalomyelitis. Epub 2019/04/27 PloS One 14 (4), e0215981. https://doi.org/10.1371/journal.pone.0215981. PubMed PMID: 31026283; PMCID: PMC6485712.

Agliardi, C., Guerini, F.R., Zanzottera, M., Rovaris, M., Caputo, D., Clerici, M., 2017. Indoleamine-2,3-dioxygenase(IDO)2 polymorphisms are not associated with multiple sclerosis in Italians. Epub 2017/05/10 J. Neurol. Sci. 377, 31–34. https://doi.org/10.1016/j.jns.2017.03.048. PubMed PMID: 28477703.

Albini, E., Rosini, V., Gargaro, M., Mondanelli, G., Belladonna, M.L., Pallotta, M.T., Volpi, C., Fallarino, F., Macchiarulo, A., Antognelli, C., Bianchi, R., Vacca, C., Puccetti, P., Grohmann, U., Orabona, C., 2017. Distinct roles of immunoreceptor tyrosine-based motifs in immunosuppressive indoleamine 2,3-dioxygenase 1. Epub 2016/10/04 J. Cell Mol. Med. 21 (1), 165–176. https://doi.org/10.1111/jcmm.12954. PubMed PMID: 27696702; PMCID: PMC5192792.

Albini, E., Coletti, A., Greco, F., Pallotta, M.T., Mondanelli, G., Gargaro, M., Belladonna, M.L., Volpi, C., Bianchi, R., Grohmann, U., Macchiarulo, A., Orabona, C., 2018. Identification of a 2-propanol analogue modulating the non-enzymatic function of indoleamine 2,3-dioxygenase 1. Epub 2018/11/06 Biochem. Pharmacol. 158, 286–297. https://doi.org/10.1016/j.bcp.2018.10.033. PubMed PMID: 30391205.

Baban, B., Chandler, P., McCool, D., Marshall, B., Munn, D.H., Mellor, A.L., 2004. Indoleamine 2,3-dioxygenase expression is restricted to fetal trophoblast giant cells during murine gestation and is maternal genome specific. Epub 2004/04/06 J. Reprod. Immunol. 61 (2), 67–77. https://doi.org/10.1016/j.jri.2003.11.003. PubMed PMID: 15063630.

Barr, T.A., Shen, P., Brown, S., Lampropoulou, V., Roch, T., Lawrie, S., Fan, B., O'Connor, R.A., Anderton, S.M., Bar-Or, A., Fillatreau, S., Gray, D., 2012. B cell

depletion therapy ameliorates autoimmune disease through ablation of IL-6-producing B cells. Epub 2012/05/02 J. Exp. Med. 209 (5), 1001–1010. https://doi.org/10.1084/jem.20111675. PubMed PMID: 22547654; PMCID: PMC3348102.

Brooks, A.K., Lawson, M.A., Rytych, J.L., Yu, K.C., Janda, T.M., Steelman, A.J., McCusker, R.H., 2016. Immunomodulatory factors galectin-9 and Interferon-gamma synergize to Induce expression of rate-limiting enzymes of the kynurenine pathway in the mouse Hippocampus. Epub 2016/11/02 Front. Immunol. 7, 422. https://doi.org/10.3389/fimmu.2016.00422. PubMed PMID: 27799931; PMCID: PMC5065983.

Brooks, A.K., Lawson, M.A., Smith, R.A., Janda, T.M., Kelley, K.W., McCusker, R.H., 2016. Interactions between inflammatory mediators and corticosteroids regulate transcription of genes within the Kynurenine Pathway in the mouse hippocampus. Epub 2016/05/05 J. Neuroinflammation 13 (1), 98. https://doi.org/10.1186/s12974-016-0563-1. PubMed PMID: 27142940; PMCID: PMC4855471.

Brooks, A.K., Janda, T.M., Lawson, M.A., Rytych, J.L., Smith, R.A., Ocampo-Solis, C., McCusker, R.H., 2017. Desipramine decreases expression of human and murine indoleamine-2,3-dioxygenases. Brain Behav. Immun. 62, 219–229. https://doi.org/10.1016/j.bbi.2017.02.010. PubMed PMID: 28212884; PMCID: PMC5382643.

Cha, L., Jones, A.P., Trend, S., Byrne, S.N., Fabis-Pedrini, M.J., Carroll, W.M., Lucas, R.M., Cole, J.M., Booth, D.R., Kermode, A.G., Hart, P.H., 2018. Tryptophan and arginine catabolic enzymes and regulatory cytokines in clinically isolated syndrome and multiple sclerosis. Epub 2018/08/22 Clin. Transl. Immunol. 7 (8), e1037. https://doi.org/10.1002/cti2.1037. PubMed PMID: 30128151; PMCID: PMC6095938.

Chen, W.I.D.O., 2011. More than an enzyme. Epub 2011/08/20 Nat. Immunol. 12 (9), 809–811. https://doi.org/10.1038/ni.2088. PubMed PMID: 21852775.

Compston, A., Coles, A., 2008. Multiple sclerosis. Epub 2008/10/31. doi: S0140-6736(08)61620-7 [pii] Lancet 372 (9648), 1502–1517. https://doi.org/10.1016/S0140-6736(08)61620-7 [doi]. PubMed PMID: 18970977.

Delgoffe, G.M., Pollizzi, K.N., Waickman, A.T., Heikamp, E., Meyers, D.J., Horton, M.R., Xiao, B., Worley, P.F., Powell, J.D., 2011. The kinase mTOR regulates the differentiation of helper T cells through the selective activation of signaling by mTORC1 and mTORC2. Epub 2011/03/02 Nat. Immunol. 12 (4), 295–303. https://doi.org/10.1038/ni.2005. PubMed PMID: 21358638; PMCID: PMC3077821.

Donia, M., Mangano, K., Amoroso, A., Mazzarino, M.C., Imbesi, R., Castrogiovanni, P., Coco, M., Meroni, P., Nicoletti, F., 2009. Treatment with rapamycin ameliorates clinical and histological signs of protracted relapsing experimental allergic encephalomyelitis in Dark Agouti rats and induces expansion of peripheral CD4+ CD25+Foxp3+ regulatory T cells. Epub 2009/07/25 J. Autoimmun. 33 (2), 135–140. https://doi.org/10.1016/j.jaut.2009.06.003. PubMed PMID: 19625166.

Dostal, C.R., Carson Sulzer, M., Kelley, K.W., Freund, G.G., McCusker, R.H., 2017. Glial and tissue-specific regulation of Kynurenine Pathway dioxygenases by acute stress of mice. Neurobiol. Stress 7, 1–15. https://doi.org/10.1016/j.ynstr.2017.02.002. PubMed PMID: 29520368; PMCID: PMC5840960.

Dostal, C.R., Gamsby, N.S., Lawson, M.A., McCusker, R.H., 2018. Glia- and tissue-specific changes in the Kynurenine Pathway after treatment of mice with lipopolysaccharide and dexamethasone. PubMed PMID: 29241670; PMCID: PMC5857427 Brain Behav. Immun. 69, 321–335. https://doi.org/10.1016/j.bbi.2017.12.006.

Esposito, M., Ruffini, F., Bellone, M., Gagliani, N., Battaglia, M., Martino, G., Furlan, R., 2010. Rapamycin inhibits relapsing experimental autoimmune encephalomyelitis by both effector and regulatory T cells modulation. Epub 2010/02/13 J. Neuroimmunol. 220 (1–2), 52–63. https://doi.org/10.1016/j.jneuroim.2010.01.001. PubMed PMID: 20149931.

Ganesan, S., Roy, C.R., 2019. Host cell depletion of tryptophan by IFNγ-induced Indoleamine 2,3-dioxygenase 1 (IDO1) inhibits lysosomal replication of Coxiella burnetii. Epub 2019/08/29 PLoS Pathog. 15 (8), e1007955. https://doi.org/10.1371/journal.ppat.1007955. PubMed PMID: 31461509; PMCID: PMC6736304.

Hauser, S.L., Waubant, E., Arnold, D.L., Vollmer, T., Antel, J., Fox, R.J., Bar-Or, A., Panzara, M., Sarkar, N., Agarwal, S., Langer-Gould, A., Smith, C.H., 2008. B-cell depletion with rituximab in relapsing-remitting multiple sclerosis. Epub 2008/02/15. doi: 358/7/676 [pii] N. Engl. J. Med. 358 (7), 676–688. https://doi.org/10.1056/NEJMoa0706383 [doi]. PubMed PMID: 18272891.

Hou, H., Miao, J., Cao, R., Han, M., Sun, Y., Liu, X., Guo, L., 2017. Rapamycin ameliorates experimental autoimmune encephalomyelitis by suppressing the mTOR-STAT3 pathway. Epub 2017/06/11 Neurochem. Res. 42 (10), 2831–2840. https://doi.org/10.1007/s11064-017-2296-7. PubMed PMID: 28600752.

Inoue, M., Williams, K.L., Oliver, T., Vandenabeele, P., Rajan, J.V., Miao, E.A., Shinohara, M.L., 2012. Interferon-beta therapy against EAE is effective only when development of the disease depends on the NLRP3 inflammasome. Epub 2012/05/25 Sci. Signal. 5 (225), ra38. https://doi.org/10.1126/scisignal.2002767. PubMed PMID: 22623753; PMCID: PMC3509177.

Kim, S., Steelman, A.J., Zhang, Y., Kinney, H.C., Li, J., 2012. Aberrant upregulation of astroglial ceramide potentiates oligodendrocyte injury. Epub 2011/05/28 Brain Pathol. 22 (1), 41–57. https://doi.org/10.1111/j.1750-3639.2011.00501.x. PubMed PMID: 21615590; PMCID: 4500118.

Koga, T., Hedrich, C.M., Mizui, M., Yoshida, N., Otomo, K., Lieberman, L.A., Rauen, T., Crispin, J.C., Tsokos, G.C., 2014. CaMK4-dependent activation of AKT/mTOR and CREM-alpha underlies autoimmunity-associated Th17 imbalance. Epub 2014/03/29 J. Clin. Invest. 124 (5), 2234–2245. https://doi.org/10.1172/jci73411. PubMed PMID: 24667640; PMCID: PMC4001553.

Kwidzinski, E., Bunse, J., Aktas, O., Richter, D., Mutlu, L., Zipp, F., Nitsch, R., Bechmann, I., 2005. Indolamine 2,3-dioxygenase is expressed in the CNS and down-regulates autoimmune inflammation. Epub 2005/06/09. doi: 04-3228fje [pii Faseb. J. 19 (10), 1347–1349. https://doi.org/10.1096/fj.04-3228fje. PubMed PMID: 15939737.

Lippens, C., Duraes, F.V., Dubrot, J., Brighouse, D., Lacroix, M., Irla, M., Aubry-Lachainaye, J.P., Reith, W., Mandl, J.N., Hugues, S., 2016. IDO-orchestrated crosstalk between pDCs and Tregs inhibits autoimmunity. Epub 2016/07/30 J. Autoimmun. 75, 39–49. https://doi.org/10.1016/j.jaut.2016.07.004. PubMed PMID: 27470005; PMCID: PMC5127883.

Lovelace, M.D., Varney, B., Sundaram, G., Franco, N.F., Ng, M.L., Pai, S., Lim, C.K., Guillemin, G.J., Brew, B.J., 2016. Current evidence for a role of the kynurenine pathway of tryptophan metabolism in multiple sclerosis. Epub 2016/08/20 Front. Immunol. 7, 246. https://doi.org/10.3389/fimmu.2016.00246. PubMed PMID: 27540379; PMCID: PMC4972824.

Lu, H.C., Kim, S., Steelman, A.J., Tracy, K., Zhou, B., Michaud, D., Hillhouse, A.E., Konganti, K., Li, J., 2020. STAT3 signaling in myeloid cells promotes pathogenic myelin-specific T cell differentiation and autoimmune demyelination. Epub 2020/02/26 Proc. Natl. Acad. Sci. U. S. A. 117 (10), 5430–5441. https://doi.org/10.1073/pnas.1913997117. PubMed PMID: 32094172; PMCID: PMC7071888.

Mancuso, R., Hernis, A., Agostini, S., Rovaris, M., Caputo, D., Fuchs, D., Clerici, M., 2015. Indoleamine 2,3 dioxygenase (IDO) expression and activity in relapsing-remitting multiple sclerosis. Epub 2015/06/26 PloS One 10 (6), e0130715. https://doi.org/10.1371/journal.pone.0130715. PubMed PMID: 26110930; PMCID: PMC4482492.

Matysiak, M., Stasiolek, M., Orlowski, W., Jurewicz, A., Janczar, S., Raine, C.S., Selmaj, K., 2008. Stem cells ameliorate EAE via an indoleamine 2,3-dioxygenase (IDO) mechanism. J. Neuroimmunol. 193 (1–2), 12–23. https://doi.org/10.1016/j.jneuroim.2007.07.025. PubMed PMID: 18077006; PMCID: PMC2681256.

Baltimore, Md : 1950 Merlo, L.M.F., Pigott, E., DuHadaway, J.B., Grabler, S., Metz, R., Prendergast, G.C., Mandik-Nayak, L., 2014. IDO2 is a critical mediator of autoantibody production and inflammatory pathogenesis in a mouse model of autoimmune arthritis, Epub 2014/02/04 J. Immunol. 192 (5), 2082–2090. https://doi.org/10.4049/jimmunol.1303012. PubMed PMID: 24489090; PMCID: PMC3947779.

Merlo, L.M., DuHadaway, J.B., Grabler, S., Prendergast, G.C., Muller, A.J., Mandik-Nayak, L., 2016. IDO2 modulates T cell-dependent autoimmune responses through a B cell-intrinsic mechanism. J. Immunol. 196 (11), 4487–4497. https://doi.org/10.4049/jimmunol.1600141. PubMed PMID: 27183624; PMCID: PMC4875825.

Metz, R., Smith, C., DuHadaway, J.B., Chandler, P., Baban, B., Merlo, L.M.F., Pigott, E., Keough, M.P., Rust, S., Mellor, A.L., Mandik-Nayak, L., Muller, A.J., Prendergast, G.C., 2019. IDO2 is critical for IDO1-mediated T-cell regulation and exerts a non-redundant function in inflammation. Epub 2019/06/22 Int. Immunol. 31 (3), 181–182. https://doi.org/10.1093/intimm/dxz003. PubMed PMID: 31222337; PMCID: PMC6941493.

Miller, D.H., Khan, O.A., Sheremata, W.A., Blumhardt, L.D., Rice, G.P., Libonati, M.A., Willmer-Hulme, A.J., Dalton, C.M., Miszkiel, K.A., O'Connor, P.W., 2003. A controlled trial of natalizumab for relapsing multiple sclerosis. Epub 2003/01/03 N. Engl. J. Med. 348 (1), 15–23. https://doi.org/10.1056/NEJMoa020696 [doi] 348/1/15 [pii]. PubMed PMID: 12510038.

Mondanelli, G., Coletti, A., Greco, F.A., Pallotta, M.T., Orabona, C., Iacono, A., Belladonna, M.L., Albini, E., Panfili, E., Fallarino, F., Gargaro, M., Manni, G., Matino, D., Carvalho, A., Cunha, C., Maciel, P., Di Filippo, M., Gaetani, L., Bianchi, R., Vacca, C., Iamandii, I.M., Proietti, E., Boscia, F., Annunziato, L., Peppelenbosch, M., Puccetti, P., Calabresi, P., Macchiarulo, A., Santambrogio, L., Volpi, C., Grohmann, U., 2020. Positive allosteric modulation of indoleamine 2,3-dioxygenase 1 restrains neuroinflammation. Epub 2020/02/07 Proc. Natl. Acad. Sci. U. S. A. 117 (7), 3848–3857. https://doi.org/10.1073/pnas.1918215117. PubMed PMID: 32024760; PMCID: PMC7035626.

Munn, D.H., Mellor, A.L., 2013. Indoleamine 2,3 dioxygenase and metabolic control of immune responses. Epub 2012/10/30 Trends Immunol. 34 (3), 137–143. https://doi.org/10.1016/j.it.2012.10.001. PubMed PMID: 23103127; PMCID: PMC3594632.

Negrotto, L., Correale, J., 2017. Amino acid catabolism in multiple sclerosis affects Immune homeostasis. Epub 2017/01/29 J. Immunol. 198 (5), 1900–1909. https://doi.org/10.4049/jimmunol.1601139. PubMed PMID: 28130499.

Baltimore, Md : 1950 Oliver, A.R., Lyon, G.M., Ruddle, N.H., 2003. Rat and human myelin oligodendrocyte glycoproteins induce experimental autoimmune encephalomyelitis by different mechanisms in C57BL/6 mice, Epub 2003/06/21 J. Immunol. 171 (1), 462–468. https://doi.org/10.4049/jimmunol.171.1.462. PubMed PMID: 12817031.

Orsini, H., Araujo, L.P., Maricato, J.T., Guereschi, M.G., Mariano, M., Castilho, B.A., Basso, A.S., 2014. GCN2 kinase plays an important role triggering the remission phase of experimental autoimmune encephalomyelitis (EAE) in mice. Epub 2013/12/24 Brain Behav. Immun. 37, 177–186. https://doi.org/10.1016/j.bbi.2013.12.012. PubMed PMID: 24362236.

Baltimore, Md : 1950 Parker Harp, C.R., Archambault, A.S., Sim, J., Ferris, S.T., Mikesell, R.J., Koni, P.A., Shimoda, M., Linington, C., Russell, J.H., Wu, G.F., 2015. B cell antigen presentation is sufficient to drive neuroinflammation in an animal model of multiple sclerosis, Epub 2015/04/22 J. Immunol. 194 (11), 5077–5084. https://doi.org/10.4049/jimmunol.1402236. PubMed PMID: 25895531; PMCID: PMC4433779.

Saadoun, S., Waters, P., Bell, B.A., Vincent, A., Verkman, A.S., Papadopoulos, M.C., 2010. Intra-cerebral injection of neuromyelitis optica immunoglobulin G and human complement produces neuromyelitis optica lesions in mice. Epub 2010/01/06 Brain : J. Neurol. 133 (Pt 2), 349–361. https://doi.org/10.1093/brain/awp309. PubMed PMID: 20047900; PMCID: PMC2822632.

Sakurai, K., Zou, J.P., Tschetter, J.R., Ward, J.M., Shearer, G.M., 2002. Effect of indoleamine 2,3-dioxygenase on induction of experimental autoimmune encephalomyelitis. J. Neuroimmunol. 129 (1–2), 186–196. PubMed PMID: 12161035.

Steelman, A.J., Thompson, J.P., Li, J., 2012. Demyelination and remyelination in anatomically distinct regions of the corpus callosum following cuprizone intoxication. Epub 2011/10/22 Neurosci. Res. 72 (1), 32–42. https://doi.org/10.1016/j.neures.2011.10.002. PubMed PMID: 22015947; PMCID: PMC3230728.

van den Berg, R., Laman, J.D., van Meurs, M., Hintzen, R.Q., Hoogenraad, C.C., 2016. Rotarod motor performance and advanced spinal cord lesion image analysis refine

assessment of neurodegeneration in experimental autoimmune encephalomyelitis. Epub 2016/01/20 J. Neurosci. Methods 262, 66–76. https://doi.org/10.1016/j.jneumeth.2016.01.013. PubMed PMID: 26784021.

Willenborg, D.O., Fordham, S.A., Staykova, M.A., Ramshaw, I.A., Cowden, W.B., 1999. IFN-gamma is critical to the control of murine autoimmune encephalomyelitis and regulates both in the periphery and in the target tissue: a possible role for nitric oxide. Baltimore, Md : 1950 J. Immunol. 163 (10), 5278–5286. Epub 1999/11/24. doi: ji_v163n10p5278 [pii]. PubMed PMID: 10553050.

Yeung, A.W., Wu, W., Freewan, M., Stocker, R., King, N.J., Thomas, S.R., 2012. Flavivirus infection induces indoleamine 2,3-dioxygenase in human monocyte-derived macrophages via tumor necrosis factor and NF-κB. Epub 2012/02/04 J. Leukoc. Biol. 91 (4), 657–666. https://doi.org/10.1189/jlb.1011532. PubMed PMID: 22301793.

Zhou, X., Liu, X., Liu, L., Han, C., Xie, Z., Liu, X., Xu, Y., Li, F., Bi, J., Zheng, C., 2020. Transplantation of IFN-Gamma Primed hUCMSCs Significantly Improved Outcomes of Experimental Autoimmune Encephalomyelitis in a Mouse Model. Epub 2020/03/17. Neurochemical research. https://doi.org/10.1007/s11064-020-03009-y. PubMed PMID: 32172400.